



Research Article

## Preparation, Characterisation and Evaluation of Antimicrobial Activity of Al<sup>3+</sup>-Modified Starch Nanoemulsion

Netai Mukaratirwa-Muchanyereyi<sup>1</sup>✉, Phuzile Tshuma<sup>1</sup>, Caliphs Zvinowanda<sup>2</sup>, Stephen Nyoni<sup>3</sup>

<sup>1</sup>Bindura University of Science Education, Department of Chemistry, P. Bag 1020, Bindura, Zimbabwe.

<sup>2</sup>University of Johannesburg, Department of Applied Chemistry, Doornfontein, Johannesburg, 2028, South Africa.

<sup>3</sup>Chinhoyi University of Technology, Department of Chemistry, P. Bag 7724, Chinhoyi, Zimbabwe.

✉ Corresponding author. E-mail: nmuchanyereyi@buse.ac.zw or nmuchanyereyi@gmail.com; Tel.: +263773410239

**Received:** Nov. 21, 2018; **Accepted:** Jul. 19, 2019; **Published:** Jul. 23, 2019.

**Citation:** Netai Mukaratirwa-Muchanyereyi, Phuzile Tshuma, Caliphs Zvinowanda, and Stephen Nyoni, Preparation, Characterisation and Evaluation of Antimicrobial Activity of Al<sup>3+</sup>-Modified Starch Nanoemulsion. *Nano Biomed. Eng.*, 2019, 11(3): 215-225.

**DOI:** 10.5101/nbe.v11i3.p215-225.

### Abstract

An oil-in-water nanoemulsion comprising of aluminium ions encapsulated in a chemically modified starch derivative was prepared, characterised and evaluated for the antimicrobial activity. The nanoemulsion was prepared by emulsion-coacervation method under ultrasonication conditions. Based on the aluminium oxinate chelate of Al<sup>3+</sup> ions, Al(ox)<sub>3</sub>, the encapsulation efficiency (92%) was determined by ultraviolet-visible spectrometry measured at 365 nm, and the subsequent drug loading efficiency was also calculated to be 92%. Fourier transform infrared spectroscopy confirmed the formation of carboxymethyl starch, and the degree of substitution was found to be 0.17 by back-titration, using phenolphthalein as an indicator. Transmission electron microscopy (TEM) micrographs revealed spherical nano-droplets with a minimum particle diameter of 7 nm that had coalesced to form nano aggregates of variable diameters. There was also an indication of the formation a larger nano cluster with a length of approximately 215 nm. Freeze-thaw cycles revealed that the nanoemulsion was stable. Disc diffusion method was used to evaluate the antimicrobial activity of the synthesized aluminum ion nanoemulsion on selected gram-negative bacteria (*E. coli* and *P. aeruginosa*) and gram-positive bacteria (*B. subtilis* and *S. aureus*).

**Keywords:** Aluminium nanoemulsion; Encapsulation efficiency; Antimicrobial activity

### Introduction

Nanomedicine is becoming an exciting and promising field that is contributing to the continued search for better medications to counter antibiotic resistance strains of bacteria, and nanoparticles have already been applied as drug delivery systems with great success [1]. Nanoemulsions have also been found to possess a key function in nanomedicine. A nanoemulsion is a true emulsion with droplets of 20-200 nm in diameter, consisting of two

immiscible liquid phases, one is hydrophobic, and the other is hydrophilic [2]. Nanoemulsions for medical applications are generally composed of a biodegradable polymeric nanoparticle core, which can encapsulate active agents, and a stabilizing outer layer for solubilisation in aqueous solution [3]. Nano emulsions are known to be kinetically stable; hence, they've been applied in nanomedical fields [4, 5]. In this study, we report antibacterial activity of Al<sup>3+</sup>-modified starch nanoemulsion. Starch has been selected because of the hydroxyl groups on its glucose

units which are potential coordination centres for metal ion ligands; it is also safe (non-toxic), cheap, as well as biocompatible [6]. Starch is also modified since it is insoluble in cooled water and tends to retrograde [7]. In this work, cross-linked carboxymethyl starch (CCMS) was used to encapsulate  $Al^{3+}$ , since carboxymethylation and cross-linking are known to activate the starch. Carboxymethyl starch (CMS) is considered a green polymer with great importance in medicine as well as in other fields like cosmetics, food industry, and many other industrial applications [8]. Furthermore, the antimicrobial properties of alumina (aluminium oxide) nanoparticles are well documented, but studies on the antibacterial role of aluminium ions, encapsulated in a polymeric nanoemulsion, have not been reported. The use of modified starch to encapsulate aluminium ions is to promote sustained release of the aluminium ions from a biologically safe CMS. This research work is therefore focused on the synthesis, characterisation and evaluation of the antimicrobial activity of aluminium ion nanoemulsion on selected gram-negative bacteria (*E. coli* and *P. aeruginosa*) and gram-positive bacteria (*B. subtilis* and *S. aureus*). Encapsulation of hydrophilic molecules is a major scientific challenge, as most literature has focused on hydrophobic compounds [9]. Use of a natural polymer derivative, CMS, to encapsulate the highly hydrophilic  $Al^{3+}$  ion is therefore a new research course.

## Experimental

### Materials

Starch soluble (chemical pure) glacial acetic acid (99%, analytical reagent, and citric acid monohydrate (99.5%, CP) were purchased from Associated Chemical Enterprises (South Africa). Triton X-114 was supplied by Sigma-Aldrich. 8-Hydroxyquinoline (99%) from Riedel-de Han, South Africa. Liquid paraffin was purchased from a local pharmacy and disodium hydrogen orthophosphate 99% from UniLab (South Africa). Hydrochloric acid 32% was purchased from Minema (South Africa), Sodium hydroxide pellets (98%) and granular aluminium sulphate (99%) from Glassworld (South Africa). Monochloroacetic acid (MCA) (99%) was purchased from Himedia (India). Isopropanol and methanol were of AR grade and were all used without further purification.

### Equipment

The shape and morphology of nanoemulsion

particles were studied by transmission electron microscopy (JEOL JEM-2100, Japan) at an accelerating voltage of 200.00 kV and beam current of 102  $\mu$ A. Attenuated total reflectance (ATR) FTIR analyses were performed on a Nicolet iS5 spectrometer (Thermo Fischer Scientific) using the iD7 ATR accessory with diamond crystal (resolution 4  $cm^{-1}$ ; scan rate of 16 scans per second and bandwidth 4000–400  $cm^{-1}$ ). The resulting spectra were converted using the software OMNIC<sup>®</sup>. Analyses were done on the soluble starch, carboxymethyl starch (CMS), acidified carboxymethyl starch (H-CMS) and the nanoemulsion. Ultrasonic water bath sonicator (Japson, India) was used for ultrasound assisted crosslinking. Thermo Fischer Scientific GENESYS 10S ultraviolet-visible spectrometry (UV-Vis) spectrophotometer was used for all UV-Vis analyses.

### Synthesis of carboxymethyl starch (CMS)

CMS was synthesized using the solvent slurry method according to one method described in the work by Spsychaj and coworkers [10]. About 20 g of starch soluble ( $C_6H_{10}O_5$ )<sub>n</sub> was mixed with 80 mL of isopropanol (4 mL/g of starch) and 4 g of NaOH (dissolved in 6 mL distilled water). The mixture was heated in a water bath at 45 °C for 45 min, with occasional stirring using a glass rod. At the end of 45 min, 4.87 g of MCA (NaOH : MCA mole ratio of 1.94) dissolved in minimal isopropanol solvent was added and the heating continued for another 100 min.

The solvent was then removed using a rotary evaporator. The resultant thick, lumpy solid was re-suspended in 150 mL of distilled water, and the pH neutralized with glacial acetic acid. Solid CMS was re-precipitated with 200 mL cold methanol.

The supernatant was decanted into a reagent bottle and stored overnight in a freezer, while the sample was left at room temperature. The next morning, 30 mL of cold methanol was poured onto the sticky paste, after which it became a white granular solid that was easier to handle.

The solid was then filtered and dried under vacuum. The residue was purified by washing with cold methanol until the conductivity of the filtrate was about 2  $\mu$ S. The sample was left to dry at room temperature over a six-day period. After drying, carboxymethyl starch (15.80 g) was obtained.

Dry sample granules were ground using a pestle

and mortar and passed through a 250  $\mu\text{m}$  sieve before storage [11, 12].

## Determination of the degree of substitution (DS)

The degree of substitution was determined by titration as follows:

### Sample pretreatment

1 g of dry CMS sample was acidified by dispersing in 10 mL of 0.2 M HCl. The solid was re-precipitated with cold methanol and filtered. Excess acid was removed by first washing with a small volume of 80:20 v/v cold methanol: water solution. Thereafter, the precipitate was washed with distilled water until the filtrate had little effect on a strip of blue litmus paper. The granules were then dried, ground using a pestle and mortar and passed through a 235  $\mu\text{m}$  sieve.

### DS determination by back-titration

0.5 g (0.1 mg) of H-CMS was dissolved in 25 mL of 0.2 M NaOH. This solution was transferred to a 250 mL volumetric flask and filled up to the mark with distilled water.

25 mL aliquots of the solution were transferred to Erlenmeyer flasks and the excess NaOH titrated with 0.2 M HCl using phenolphthalein as an indicator. An average value of three titrations was used for calculations. A blank titration containing only NaOH was also done.

## Synthesis of $\text{Al}^{3+}$ -cross linked carboxymethyl starch (CCMS) nano-emulsion

Synthesis of  $\text{Al}^{3+}$ -CCMS nanoemulsion was done in three stages, namely (i) formation of a w/o emulsion, (ii) ultra-sound assisted crosslinking, and (iii) formation of a w/o/w nanoemulsion.

### W/o emulsion

To formulate the organic phase, 0.5 mL of Triton X-114 was added to 20 mL of liquid paraffin in a 250 mL conical flask, with continuous magnetic stirring. 10 mL of a 1:1 v/v mixture of aqueous  $\text{Al}^{3+}$  (1000 mg/L, pH = 2) and 1% CMS (pH = 8.41) were delivered drop-wise from a burette into the stirred organic phase over 3–5 min. The mixture was magnetically stirred at 55 °C for 60 min.

### Ultra-sound assisted crosslinking

The emulsion separated into three distinct layers upon standing at room temperature for a few minutes. It was transferred to ultrasonic water bath sonicator (Japson, India) in that state and ultra-sonication started. The temperature of the bath ranged from 58 °C up to 74 °C. 10 mL of a mixture of 5% w/v citric acid and the catalyst  $\text{Na}_2\text{HPO}_4$  were then added drop-wise from a burette over a 40-min period. Ultra-sonication was continued for 60 min.

### Dispersion stability test of nanoemulsion

The nanoemulsion was first subjected to centrifugation to eliminate creaming followed by freeze-thaw cycles for at least 48 h. This was to ensure that it was stable and not metastable.

**Centrifugation:** The diluted nanoemulsion was centrifuged at 2500 rpm for 30 min, with further intermediary dilution until the formulation no longer showed any phase separation and/or creaming. The sample that “passed” was then taken for the freeze/thaw stress test.

**Freeze/thaw cycles:** Three freeze/thaw cycles were done between  $-4$  °C and  $+25$  °C with storage at each temperature for a minimum period of 48 h.

## Characterisation

### Characterisation of the o/w nanoemulsion by ultraviolet-visible spectrometry (UV-Vis)

Encapsulation efficiency and drug loading efficiency (DLE) of the complex were investigated by UV-Vis. Drug loading of the nanoemulsion was measured by dissolving the aluminium oxinate precipitate in phosphate buffered saline (PBS), before diluting with distilled water. The drug content was determined at 365 nm.

### Preparation of standard solutions

Standard solutions of the  $\text{Al}^{3+}$ -CCMS nanoemulsion that absorbed between 0 and 1 were prepared by serial dilution as follows:

1000  $\mu\text{L}$  (containing 1 mg of  $\text{Al}^{3+}$ ) of the 1000 mg/L stock solution was pipetted into a 50 mL volumetric flask, and the excess oxine (equivalent to 350  $\mu\text{L}$ ) was added to form the aluminium oxinate complex. This solution was warmed in a water bath until there was visible precipitation of the aluminum oxinate. The precipitate was re-dissolved by adding 2 mL of PBS (pH 2) and the solution made to the mark with distilled water. 4 mL aliquot of this solution was made to 50

mL with distilled water,  $[Al^{3+}] = 1.6 \mu\text{g/mL}$ . Serial dilution of this secondary standard gave concentrations equivalent to 0.8; 0.4; 0.2 and 0.1  $\mu\text{g/mL}$ . A calibration curve was created by measuring absorbance of the five standards at 365 nm, against distilled water blank.

Sample concentration of  $Al^{3+}$  was determined in a similar way by diluting 2.5, 1.25 and 1 mL of the nanoemulsion in a 50 mL volumetric flask, (corresponding to 20, 40 and 50 times dilution).

### Encapsulation efficiency / Drug content of nanoemulsion

Drug entrapment efficiency was estimated using Equation (1) [13, 14]:

$$\text{Encapsulation efficiency (\%)} = \frac{\text{Amount of drug loaded}}{\text{Total drug amount}} \times 100. \quad (1)$$

### Drug loading efficiency (DLE)

The DLE was calculated by finding the difference between the total amount used in the formulation and the amount of free drug (Equations (2) and (3)) [13, 15].

$$\text{DLE (\%, w/w)} = \frac{\text{Amount of drug loaded}}{\text{Amount of nanocapsules}} \times 100, \quad (2)$$

$$\begin{aligned} \text{Amount of drug loaded} = \\ \text{Amount of drug used in formulation} - \text{Amount of free drug.} \end{aligned} \quad (3)$$

The amount of free  $Al^{3+}$  in the formulation was determined spectrophotometrically at 365 nm.

### Particle shape and morphology

An excess amount of 5% w/v solution of oxine dissolved in glacial acetic acid was added to an aliquot of the nanoemulsion solution. An aliquot of the resultant solution was placed on a carbon-coated copper grid, and some ethanol was added to aid drying under ambient conditions. Transmission electron microscope (TEM) images were then recorded.

### Antibacterial assay

Three sets of diffusion discs that were previously soaked in buffer solutions of pH 2, 4.5 and 6 for 30 min were spiked with nanoemulsion concentrations equivalent to 5, 10 and 15  $\mu\text{L/mL}$  and further soaked for at least 5 h before being placed on bacterial agar plates for microbial evaluation. For comparison, an antibiotic disc of a standard antibacterial agent, Kanamycin, was included as a control.

### Preparation of bacterial media

All preparations were done on a workbench previously disinfected with ethanol (96%).

### Preparation of bacterial growth media

The bacterial growth media were prepared by dissolving specific masses of the commercially available MacConkey agar (MA), nutrient agar (NA) and mannitol salt agar (MSA) (HiMedia) in 1000 mL of distilled water. The solutions were heated to boiling with occasional stirring to aid dissolution. While still hot, the MA, NA and MSA solutions were plugged with cotton wool and covered with aluminium foil before being autoclaved at 15 lbs pressure at 121 °C for 15 min. The autoclaved media were mixed well and poured onto 100 mm petri-plates (25-30 mL/plate) while still molten.

### Preparation of bacterial culture media

Two bacteria culture media were prepared by boiling (to dissolve the medium completely): Nutrient broth (NB) for *P. aeruginosa*, *E. coli* and *B. subtilis*, and mannitol selenite broth base (MSB) for *S. aureus*. The NB and MSB solutions were dispensed in separate sets of five, 20 mL vials and sterilized in a boiling water bath for 10 min before being autoclaved at 15 lbs/in<sup>2</sup> pressure (121 °C) for 15 min, followed by cooling to room temperature. The culture media were then seeded with respective bacterial strains and incubated for 24 h at a set temperature of 37 °C.

### Antimicrobial evaluation

The antibacterial effect of varied concentration of the  $Al^{3+}$ -CCMS nanoemulsion at different pH values was investigated by disc diffusion method. The diameter of zone of inhibition was measured in millimeters (mm). Two Gram-negative (G<sup>-</sup>) bacterial strains, *E. coli* and *P. aeruginosa*, and two Gram-positive (G<sup>+</sup>) strains, *B. subtilis* and *S. aureus*, used in the present research were cultured by the Biology Department at Bindura University of Science Education (BUSE).

Agar plates prepared as described in the previous section and the test microorganisms were inoculated by the spread plate method. Each soaked filter paper disc was then transferred to the agar plates and pressed down to ensure complete contact with the agar surface. At each stage, the inoculating loop was sterilized by soaking in ethanol and heating in a burner flame.

The plates were incubated overnight and the zones of inhibition (inclusive of the disc diameter, 6 mm)

around each disc measured.

## Results and Discussion

### Synthesis of carboxymethyl starch (CMS)

Fine, free-flowing white sediment settled to the bottom of the 500 mL round-bottomed flask upon mixing isopropanol and alkalizing with NaOH. This was before commencing heating in a water bath. The solvent remained as a clear supernatant. The sediment was activated starch. Addition of monochloroacetic acid after 45 min of initial heating resulted in the formation of a fluffy, copious, white solid that had the appearance of curds of thick milk. After roto-evaporation, the solid had formed into a lump with some of it sticking onto the sides of the round-bottomed flask. This was re-suspended in 150 mL of distilled water and the solution pH adjusted from 11.81 to neutral (7.02) with glacial acetic acid. As the pH was being lowered, all the undissolved small solid lumps completely dissolved. Adding cold methanol (200 mL) re-precipitated the CMS into the initial fluffy-white, copious solid. The dry white granular CMS was ground into a free-flowing powder with particles less than 250  $\mu\text{m}$ . The recovered yield of CMS was 16 g, *ca.* The degree of substitution (DS) can be improved through derivatization procedure i.e. to obtain CMS of higher DS, the CMS obtained above can be reacted again by repeating the whole procedure twice or three times [16].

### Degree of substitution (DS)

The degree of substitution was determined using Equations (4) and (5) [17]:

$$n_{\text{COOH}} = (V_b - V) \times C_{\text{HCl}} \times 10, \quad (4)$$

$$\text{DS} = (162 \times n_{\text{COOH}}) / (m_{\text{ds}} - 58 \times n_{\text{COOH}}), \quad (5)$$

where,  $n_{\text{COOH}}$  is the number of moles of carboxymethyl substituent,  $V_b$  and  $V$  are the volumes of HCl (mL) consumed for titration of blank and sample, respectively.  $C_{\text{HCl}}$  ( $\text{mol}/\text{dm}^3$ ) is the concentration of hydrochloric acid, 162 is the molar mass of anhydrous glucose unit (AGU) in  $\text{g}/\text{mol}$ ,  $m_{\text{ds}}$  (g) is the mass of dry CMS estimated from known mass of sample, 58 ( $\text{g}/\text{mol}$ ) is the increase in mass of AGU for each carboxymethyl substituent, and 10 is the ratio of total solution volume and the volume taken for titration (250/25 mL).

Thus,  $n_{\text{COOH}} = (2.6 - 2.5) \times (0.2 \text{ mol} \times 10^{-3} \text{ mL}) \times 10 = 2 \times 10^{-4} \text{ mol}$ .

$$\text{DS} = (162 \times n_{\text{COOH}}) / (m_{\text{ds}} - 58 \times n_{\text{COOH}}) = (162 \times 2 \times$$

$$10^{-4}) / (0.2 - 58 \times 2 \times 10^{-4}) = 0.172 \text{ (to 3 s.f.)}$$

Although the calculated value of the degree of substitution compares well with most literature data where values of 0.14, 0.48 and 0.92 have been reported after derivatizing once, twice and three times; respectively, the result had significant difference from the 1.36 for the adapted optimal carboxymethylation conditions reported by Spychaj and other researchers [10, 11, 16]. Also, according to Spychaj and coworkers, commercially available CMSs often exhibit low DS values up to *ca.* 0.3 [8]. It is likely that a higher value of DS could have been achieved through derivatization procedure. However, this low DS value had little effect on the encapsulation efficiency which was still high at 92%. Kim and Lim demonstrated in their work that low DS for corn starch (0.08), at moderately acidic conditions, resulted in more effective adsorption of the heavy ions Pb, Hg, Cd and Cu from water (over 99% Hg and Cd removed) [18]. This was attributed to the lower solubility of lowly-substituted CMS. While carboxymethylation activates the starch, cross-linking causes the CMS to become a relatively insoluble metal scavenger for the cations. Non-uniform breakdown of the starch molecules may also affect the DS and the molecular weight distribution of CMS [16]. This could have been the case in this work.

### Fourier-transform infrared spectroscopy (FTIR) analysis

The ATR FTIR spectra for CMS, H-CMS and starch are shown in Fig. 1.

The typical fingerprint pattern for native starch, in the region of 900 and 1300  $\text{cm}^{-1}$  was preserved in CMS samples. The CMS carboxylate ( $-\text{COO}-$ ) gave the strong bands at about 1600, 1440 and 1325  $\text{cm}^{-1}$  [10]. The increase in the  $-\text{OH}$  bending vibration and  $-\text{O}-$  stretch between 1400-1500  $\text{cm}^{-1}$  confirmed that carboxymethylation had taken place to produce CMS. Carboxymethylation was also confirmed by the decreased intensity of the  $\text{O}-\text{H}$  stretching vibration (between 3100 and 3500  $\text{cm}^{-1}$ ), due to the disruption to hydrogen bonding involving hydroxyl groups on the starch molecules; and the decreased intensity of the  $-\text{CH}_2$  symmetrical stretching vibration at approximately 3125  $\text{cm}^{-1}$  [10].

The carbonyl ( $-\text{C}=\text{O}$ ) stretch at approximately 1750  $\text{cm}^{-1}$  is evidence of protonated carboxylic groups ( $-\text{COOH}$ ) in H-CMS (confirms acidification of CMS). Table 1 summarises the characteristic functional groups on the FTIR spectra.

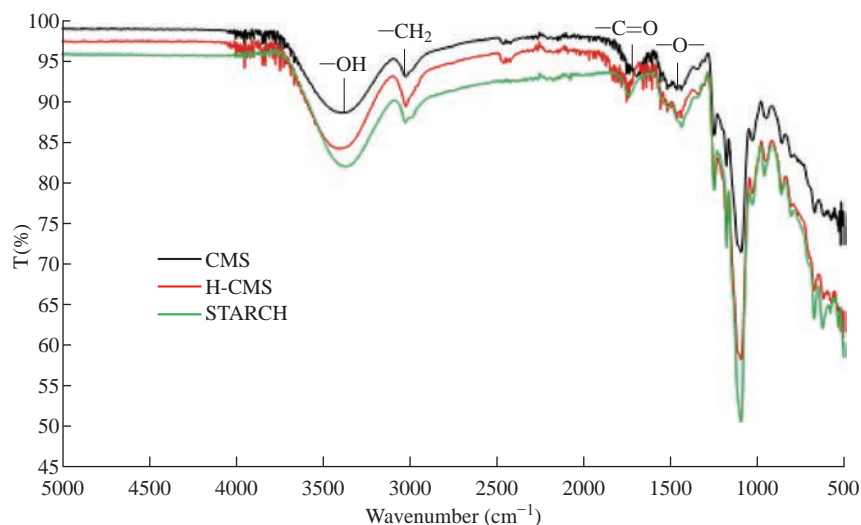


**Fig. 1** FTIR spectra for CMS, H-CMS and starch.

**Table 1** FTIR bands

Frequency (cm <sup>-1</sup> )	Bond	Compound type	References
3297.94, 3269.26	O-H	Alcohols	[19]
3125	CH <sub>2</sub>	Alkanes	[10]
1750	C=O	Carbonyl groups	[19]
1336.29 and 1338.59	-COO-	Carboxyl	[10]

### Synthesis of Al<sup>3+</sup>-CCMS nanoemulsion

At the end of the first hour under sonication, the milky white o/w coarse emulsion had separated into a white precipitate in the aqueous phase and an oil phase on top (Fig. 2(a)). After a further 1 h of sonication the emulsion became homogenous and had a very clean white appearance (Fig. 2(b)).

Although the emulsion was left in a separating funnel for approximately 18 h, there was no sign of solid sediment observed. This suggested that the emulsion might be very stable. On further storage over

at least 30 days, the nanoemulsion did not separate suggesting that the o/w emulsion was indeed stable. Furthermore, the Al<sup>3+</sup>-CCMS nanoemulsion formed as a white creamy layer on top of the bulk aqueous phase but could easily re-mix with the aqueous phase on slight agitation. Dilution of the nanoemulsion with intermediary centrifugation was done until negligible creaming was observed. Negligible creaming occurred when the nanoemulsion had been diluted 1000-fold. Encapsulation of Al<sup>3+</sup> is assumed to be through dative entrapment of the ions in the CCMS network in addition to the primary chemical adsorption. It is

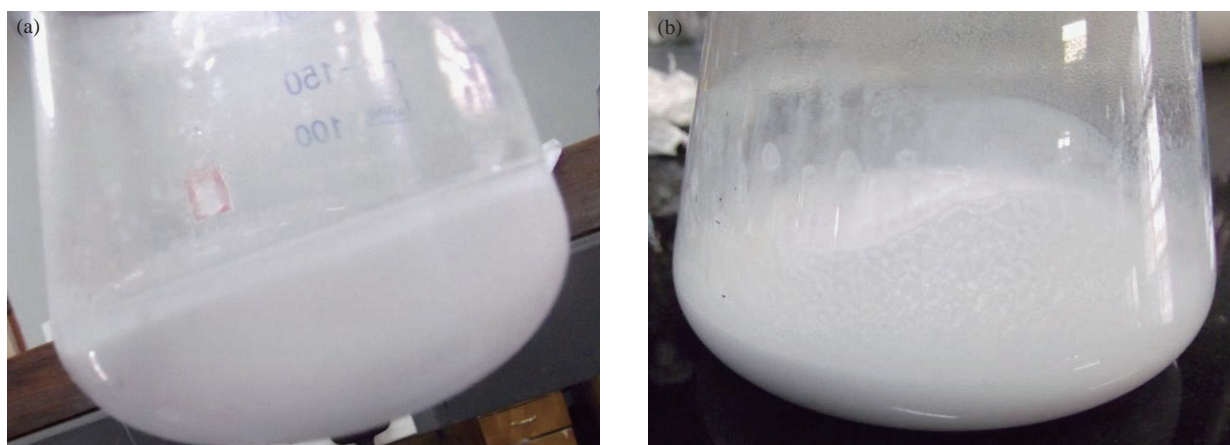


**Fig. 2** Appearance of the coarse emulsion: (a) After 1-h sonication; (b) Homogenous coarse emulsion.

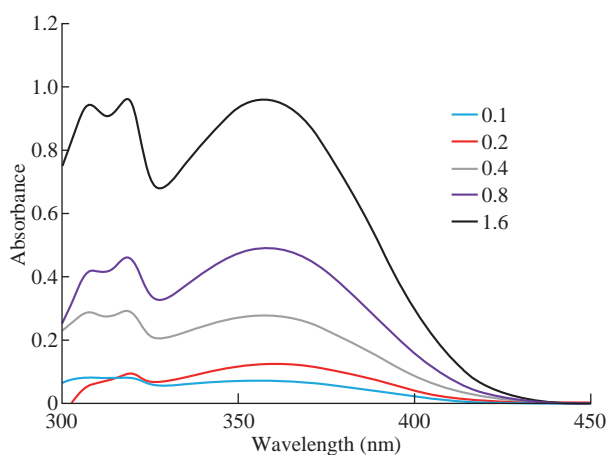
also assumed that exactly 1 mol  $\text{Al}^{3+}$  ion interacts via electrostatic bonds with carboxylic groups of the carboxymethyl moieties [20].

### UV-Vis analysis of $\text{Al}^{3+}$ -CCMS nanoemulsion

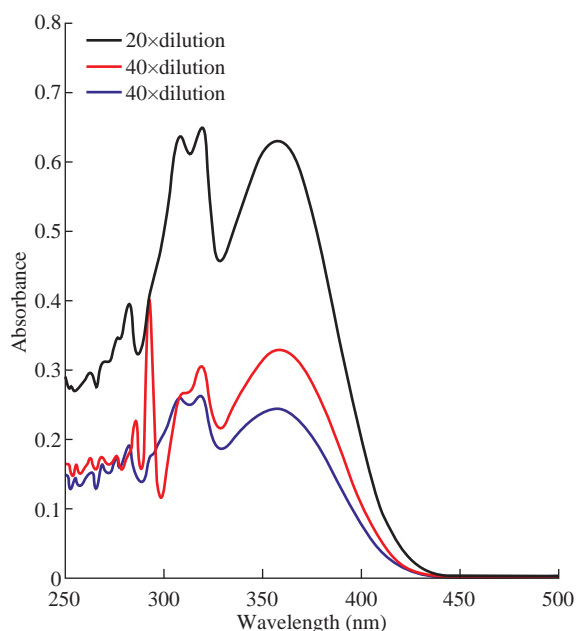
Fig. 3 shows the absorption spectra, respectively, of aluminium oxinate standard solutions, determined at 365 nm. The absorption spectra are typical of those reported by Gharbi and Jamoussi [21].

Fig. 4 below shows that the absorbance of aluminium oxinate increased with concentration, with  $\lambda_{\text{max}}$  of 357 nm, at 20 times dilution of the nanoemulsion. The peaks at approximately 318 nm are due to excess oxine.

The following calculations were performed to obtain



**Fig. 3** UV-Vis absorption spectra of aluminium oxinate standards.



**Fig. 4** UV-Vis absorption spectra of 20, 40 and 50 times dilution of the nanoemulsion sample solution.

the encapsulation efficiency (Equation (1)):

Average mass of  $\text{Al}^{3+}$  in 50 mL nanoemulsion =  $(20.236 + 21.368 + 19.645) / 3 = 20.42 \mu\text{g}$  (to 2 dp) = 0.02 mg.

Therefore, Average quantity of “free”  $\text{Al}^{3+}$  in 1000 mL nanoemulsion =  $1000 \text{ mL} / 50 \text{ mL} \times 0.02 \text{ mg} = 0.4 \text{ mg}$ , and Encapsulation efficiency (%) =  $(\text{Amount of drug loaded} / \text{Total drug amount}) \times 100 = (5 \text{ mg} - 0.4 \text{ mg}) / 5 \text{ mg} \times 100 = 92\%$ \*, \* refers to the non-encapsulated  $\text{Al}^{3+}$  ions. Using Equation (2), DLE and DLC were calculated as follows:

Drug loading capacity (DLC) =  $(\text{Amount of encapsulated drug} / \text{Total weight of drug + Polymer used})$

$\text{DLC}_{\text{theoretical}} (\%) = \text{Loaded drug (mg)} / (\text{CMS} + \text{loaded drug}) \times 100 = 10 \text{ mg} / (100 \text{ mg} + 10 \text{ mg}) \times 100 = 9.09\%$ ,  $\text{DLC}_{\text{actual}} (\%) = \text{Encapsulated drug (mg)} / (\text{CMS} + \text{loaded drug}) \times 100 = 9.2 \text{ mg} / (100 \text{ mg} + 10 \text{ mg}) \times 100 = 8.36\%$ , and  $\text{DLE} (\%) = \text{DLC}_{\text{actual}} / \text{DLC}_{\text{theoretical}} \times 100 = 8.36 / 9.09 \times 100 = 91.97\% = 92\%$ .

The high encapsulation efficiency (92%) determined in this work is characteristic of lowly-substituted and highly cross-linked CMS [18]. Thus, a low DS value (0.17) was advantageous in this case since it caused CMS to be less soluble in water. Ultrasound-assisted cross-linking of the polymer matrix may have contributed to a more water-insoluble organic phase with entrapped  $\text{Al}^{3+}$  ions.

### TEM analysis

The TEM micrograph in Fig. 5 suggests that sizes of the particles were around 7 nm (indicated with an arrow on Fig. 5).

Individual particles were spherical in shape. The

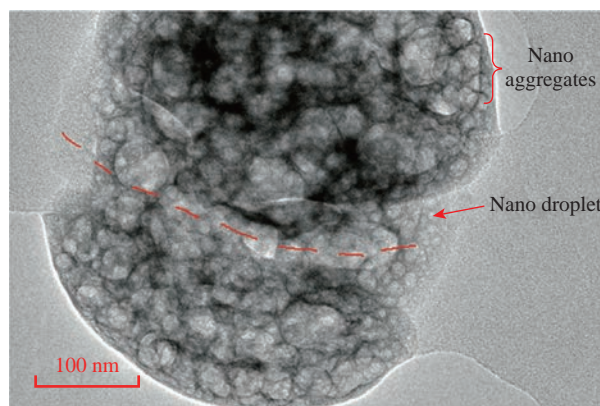


**Fig. 5** TEM micrograph of oxine-complexed “nano cluster” of the o/w nanoemulsion particles.

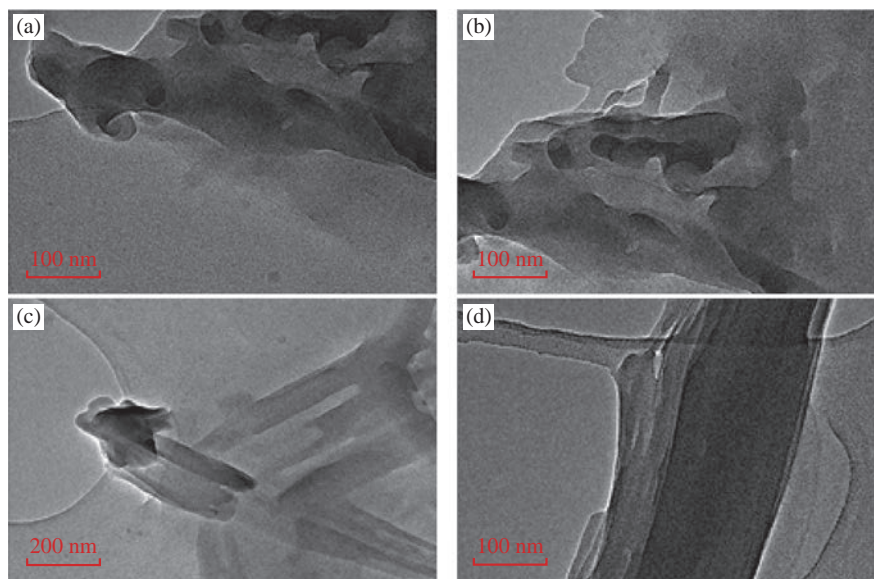


**Fig. 6** TEM images from the continuous aqueous phase.

micrograph also suggests that the nanoparticles coalesced and formed large aggregates (indicated by brace) that consequently clustered to form an even larger aggregate of approximately 215 nm at length. The  $\text{Al}^{3+}$ -CCMS nanoparticles most likely coalesced through electrostatic attraction of oxine by  $\text{Al}^{3+}$  ions in CCMS. Coalescence was promoted by the increase in the viscosity of the nanoemulsion solution as solvent evaporated during drying in the sample pre-treatment process [4]. Also, the introduction of oxine to associate with  $\text{Al}^{3+}$ -CCMS through possible chelation with  $\text{Al}^{3+}$  ions lowers the interfacial tension between the oil droplets making them more prone to coalescence [22].

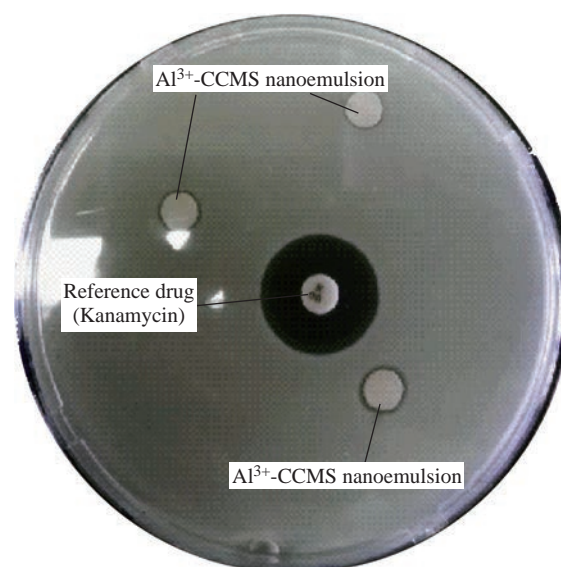
The existence, at the periphery of the larger aggregate, of a few single nano droplets with their interfacial boundary still intact shows that the concentration of the emulsifier (Triton X-114) was enough to create an intact boundary before the disruption and thinning of the liquid film. The larger nano cluster appears to have formed from two other large aggregates (indicated by broken red line on micrograph), suggesting that the composite aggregates may have coalesced at different regions in the nanoemulsion solution beforehand and then amalgamated to form the nano cluster.

Fig. 6 (a)-(d) shows some of the TEM images from the continuous aqueous phase.

The TEM images in Fig. 6(a)-(d) show inconclusive evidence of any nano droplets in the continuous aqueous phase. The structures shown are possibly due to excess oxine in acetic acid solution.

### Antimicrobial assay

After incubation at 37 °C for 24 h, the resulting zones of inhibition were uniformly circular. The measured diameters of the zones of complete inhibition at different pH values and concentrations are illustrated in Fig. 7.



**Fig. 7** The antibacterial activity of  $\text{Al}^{3+}$ -CCMS nanoemulsion against *B. subtilis*.

The zones of inhibition are summarised in Table 3 (a)-(e).

Bacterial species' susceptibility to the nanoemulsion did not correlate with susceptibility to a particular class (Gram negative or Gram positive). For both *B. subtilis*

**Table 3** Antimicrobial activity of the Al<sup>3+</sup>-CCMS nanoemulsion

<b>(a) pH = 2</b>					
*Mean zone of inhibition/mm $\pm$ 0.10					
Bacterium name	5 $\mu$ l/mL	10 $\mu$ l/mL	15 $\mu$ l/mL	† Control	
<i>Pseudomonas aeruginosa</i>	9.00	10.00	7.00	21.00	
<i>Bacillus subtilis</i>	7.00	7.80	6.50	20.30	
<i>Staphylococcus aureus</i>	--	--	--	ND	
<i>Escherichia coli</i>	--	--	--	--	
<b>(b) pH = 4.5</b>					
*Mean zone of inhibition (mm) $\pm$ 0.10					
Bacterium name	5 $\mu$ l/mL	10 $\mu$ l/mL	15 $\mu$ l/mL	† Control	
<i>Pseudomonas aeruginosa</i>	7.20	6.50	7.00	21.30	
<i>Bacillus subtilis</i>	6.50	7.00	7.00	19.30	
<i>Staphylococcus aureus</i>	--	--	--	ND	
<i>Escherichia coli</i>	--	--	--	--	
<b>(c) pH = 6</b>					
*Mean zone of inhibition (mm) $\pm$ 0.10					
Bacterium name	5 $\mu$ l/mL	10 $\mu$ l/mL	15 $\mu$ l/mL	† Control	
<i>Pseudomonas aeruginosa</i>	9.00	9.70	6.70	14.00	
<i>Bacillus subtilis</i>	7.80	7.00	8.00	19.00	
<i>Staphylococcus aureus</i>	--	--	--	ND	
<i>Escherichia coli</i>	--	--	--	--	
<b>(d) <i>Bacillus subtilis</i></b>					
*Zone of inhibition (mm) $\pm$ 0.10					
	5 $\mu$ l/mL	10 $\mu$ l/mL	15 $\mu$ l/mL	Mean	† Control
pH = 2	7.00	7.80	6.50	7.10	20.30
pH = 4.5	6.50	7.00	7.00	6.83	19.30
pH = 6	7.80	7.00	8.00	7.60	19.00
Mean	7.10	7.27	7.17		
<b>(e) <i>Pseudomonas aeruginosa</i></b>					
*Zone of inhibition/mm $\pm$ 0.10					
	5 $\mu$ l/mL	10 $\mu$ l/mL	15 $\mu$ l/mL	Mean	† Control
pH = 2	9.00	10.00	7.00	6.90	21.00
pH = 4.5	7.20	6.50	7.00	6.90	21.30
pH = 6	9.00	9.70	6.70	8.47	14.00
Mean	8.40	8.73	6.90		

\*All values are means of three readings

ND = Not determined

† = Standard antibiotic (Kanamycin)

(--)= No / Negligible Inhibition

and *P. aeruginosa*, the concentration of 5  $\mu$ l/mL had the least zone of inhibition at all pH values studied. The highest recorded mean inhibition zone for *B. subtilis* was 7.8 mm at pH 6 and 5  $\mu$ l/mL concentration. For *P. aeruginosa*, a concentration of 10  $\mu$ l/mL at pH 2 gave the highest inhibition zone of 10 mm, and 8.73 mm as the highest recorded mean inhibition zone, using a concentration of 10  $\mu$ l/mL. A clove essential oil nanoemulsion showed inhibition zones of  $18 \pm 1.3$  (*B. subtilis*),  $16 \pm 1$  (*P. aeruginosa*),  $17 \pm 1.2$  (*S. aureus*) [23]. Different antibacterial activities were also reported for a nanoemulsion incorporating essential citral essential oil. Different bacterial strains

had the following zones of inhibition,  $9.4 \pm 0.5$  (*E. coli*),  $19.2 \pm 2.3$  (*S. aureus*),  $6.2 \pm 0.2$  (*P. aeruginosa*) [24]. In another study for antibacterial activity of phytosphingosine nanoemulsions, no zone of inhibition for *P. aeruginosa* among other bacterial species was reported [25]. The use of fine emulsions as antibacterial agents is still new and a promising application. There are limited reports in literature on their use for this purpose. The reasons for higher resistance of *E. coli* and *S. aureus* require further investigation. Studies regarding the mode of action of nanoemulsion in the bacterial cell need to be done. There is evidence in literature that *S. aureus* has a unique ability to quickly

respond to each new antibiotic with the development of resistance mechanism [26]. *E. coli* is also multi-resistant to drugs.

## Conclusions

The Al<sup>3+</sup>-modified starch (i.e. Al<sup>3+</sup>-CCMS) nano-emulsion with a high encapsulation efficiency (EE) of 92% was successfully prepared and determined to have a mild inhibitory effect on Gram-positive *B. subtilis* and Gram-negative *P. aeruginosa* bacteria, with a minimum inhibition concentration of 5 µl/mL at all three pH conditions of pH 2, pH 4.5 and pH 6 under test. The highest inhibitory effect was found on *P. aeruginosa* at a concentration of 10 µl/mL and pH 2. FTIR analysis on CMS (DS = 0.17) and protonated CMS confirmed the presence of typical functional groups. The calculated degree of substitution is typical of CMS prepared from high amylose corn starch using the slurry method. Analysis of the nanoemulsion by UV-Vis analysis to determine the encapsulation efficiency produced typical spectra for aluminium oxinate. TEM micrographs showed nano aggregates formed from particles as small as 7 nm. This confirmed that the nanoemulsion had been successfully prepared. However, using other types of starch as alternatives for methylation, for example cassava starch, potato starch, can be explored. Use of a broader range of microbes to test both antibacterial and antifungal activities can also be explored further.

## Acknowledgements

Authors would like to thank the Bindura University of Science Education Research and Postgraduate centre for financial assistance.

## Conflict of Interests

Authors declare no conflict of interest

## References

- [1] K. Gayatri, G. Lakshmi, and K. Preeti, Nanoparticles - An overview of preparation and characterization, novel science. *International Journal of Pharmaceutical Science*, 2012, 1: 557-562.
- [2] C. Ye, Formulation design and development of transdermal delivery system - Nanoemulsion of Schizandrol A. *National University of Singapore*, PhD thesis 2013, Singapore.
- [3] R.H. Fang, L. Zhang, Dispersion-based methods for the engineering and manufacture of polymeric nanoparticles for drug delivery applications. *Journal of Nanoengineering and Nanomanufacturing*, 2011, 1: 106-112.
- [4] T. Panagiotou, R. Fisher, Improving product quality with entrapped stable emulsions: From theory to industrial application. *Challenges*, 2012, 3: 84-113.
- [5] N. Anton, J.P. Benoit, and P. Saulnier, Design and production of nanoparticles formulated from nano-emulsion templates - A review. *Journal of Controlled Release*, 2008, 128: 185-199.
- [6] J.A. Lemire, J.J. Harrison, and R.J. Turner, Antimicrobial activity of metals: mechanisms, molecular targets and applications. *Nature Reviews Microbiology*, 2013, 11: 371-384.
- [7] Q. Chen, H. Yu, L. Wang, et al., Recent progress in chemical modification of starch and its applications. *RSC Advances*, 2015, 5: 67459-67474.
- [8] T. Spychaj, M. Zdanowicz, J. Kujawa, et al., Carboxymethyl starch with high degree of substitution: Synthesis, properties and application. *Polimery/Polymers*, 2013, 58: 501-511.
- [9] F. Ramazani, W. Chen, C.F. Van Nostrum, et al., Strategies for encapsulation of small hydrophilic and amphiphilic drugs in PLGA microspheres: State-of-the-art and challenges. *International Journal of Pharmaceutics*, 2016, 499: 358-367.
- [10] T. Spychaj, K. Wilpiszewska, and M. Zdanowicz, Medium and high substituted carboxymethyl starch: Synthesis, characterization and application. *Starch - Stärke*, 65: 22-33.
- [11] E. Assaad, Y.J. Wang, X.X. Zhu, et al., Polyelectrolyte complex of carboxymethyl starch and chitosan as drug carrier for oral administration. *Carbohydrate Polymers*, 2011, 84: 1399-1407.
- [12] O.S. Lawal, J. Storz, H. Storz, et al., Hydrogels based on carboxymethyl cassava starch cross-linked with di- or polyfunctional carboxylic acids : Synthesis, water absorbent behavior and rheological characterizations. *European Polymer Journal*, 2009, 45: 3399-3408.
- [13] F. Makita-Chingombe, H.L. Kutscher, S.L. DiTursi, et al., Poly (lactic-co-glycolic) acid-chitosan dual loaded nanoparticles for antiretroviral nanoformulations. *Journal of Drug Delivery*, 2016, 2016: 1-10.
- [14] N. Tamilselvan, C.V. Raghavan, K. Balakumar, et al., Preparation of PLGA nanoparticles for encapsulating hydrophilic drug: Modifications of standard methods and its in vitro biological evaluation. *Asian Journal of Research in Biological and Pharmaceutical Sciences*, 2014, 2: 121-132.
- [15] X. Zhai, Gelatin nanoparticles and nanocrystals for dermal delivery. PhD thesis, Freie Universität, 2014, Berlin, Germany.
- [16] S. Lee, S.T. Kim, B.R. Pant, et al., Carboxymethylation of corn starch and characterization using asymmetrical flow field-flow fractionation coupled with multiangle light scattering. *Journal of Chromatography A*, 2010, 1217: 4623-4628.
- [17] B.R. Pant, H.J. Jeon, C.I. Park, et al., Radiation-modified carboxymethyl starch derivative as metal scavenger in aqueous solutions. *Starch/Stärke*, 2010, 62: 11-17.
- [18] B.S. Kim, S.T. Lim, Removal of heavy metal ions from water by cross-linked carboxymethyl corn starch. *Carbohydrate Polymers*, 1999, 39: 217-223.
- [19] N. Mukaratirwa-Muchanyereyi, J. Moyo, and S. Nyoni, Synthesis of silver nanoparticles using wild *Cucumis anguria*: Characterisation and antibacterial activity. *African Journal of Biotechnology*, 2017, 16: 1911-1921.
- [20] T. Heinze, A. Koschella, Carboxymethyl ethers of cellulose and starch - A review. *Macromolecular Symposia*, 2005, 223: 13-19.

- [21] S. Gharbi, B. Jamoussi, Determination of aluminium with 8-hydroxyquinoline in the hemodialysis waters by liquid chromatography of reversed phase polarity. *International Journal of Science and Research*, 2014, 3: 1-8.
- [22] R.P. Patel, J.R. Joshi, An overview on nanoemulsions: A novel approach. *International Journal of Pharmaceutical Sciences and Research*, 2012, 3: 4640-4650.
- [23] M.K. Anwer, S. Jamil, E.O. Ibnoul, et al., Enhanced antibacterial effects of clove essential oil by nanoemulsion. *Journal of Oleo Science*, 2014, 64: 347-354.
- [24] W.C. Lu, P.H. Li, Preparation characterization, and antimicrobial activity of nanoemulsion incorporating citral essential oil. *Journal of Food and Drug Analysis*, 2018, 26: 82-89.
- [25] Y.Baspinar, M. Kotmakci, and I. Ozturk, Antibacterial activity of phytosphingosine nanoemulsions against bacteria and yeast. *Celal Bayar University Journal of Science*, 2018, 14: 223-228.
- [26] A. Pantosti, A. Sanchini, and M. Monaco, Mechanism of antibiotic resistance on *Staphylococcus aureus*. *Future Microbiology*, 2007, 2: 323-334.

**Copyright**© Netai Mukaratirwa-Muchanyereyi, Phuzile Tshuma, Caliph Zvinowanda, and Stephen Nyoni. This is an open-access article distributed under the terms of the Creative Commons Attribution License, which permits unrestricted use, distribution, and reproduction in any medium, provided the original author and source are credited.